Electronic Supplementary Information

Rapid and Discriminative Detection of Nitro Aromatic Compounds with High Sensitivity by Two Zinc MOFs Synthesized through Temperature-Modulated Method

Xiu-Yan Wan[ab], Fei-Long Jiang[a], Cai-Ping Liu[a], Kang Zhou[a], Lian Chen[a]*, Yan-Li Gai[a], Yan Yang[ab] and Mao-Chun Hong[a]*

[a]*Key Laboratory of Design and Assembly of Functional Nanostructures, Fujian Institute of Research on the Structure of Matter, Chinese Academy of Sciences,Fuzhou, 350002, China.*

[b] *Graduate School of the Chinese Academy of Sciences, Beijing, 100049, China.*

Computational Methods

To shed light on the mechanisms of the fluorescent spectra for two Zinc MOFs, the Density of States (DOS) properties were calculated using density functional theory (DFT) as implemented in the CASTEP code [1]. During the calculations, the structures were determined by the experimental crystallographic data. And the parameters for calculations were set as following: the generalized gradient approximation (GGA) and the Perdew–Burke–Ernzerhof (PBE) functional [2] were adopted; the type of pseudopotential is specified as the ultrasoft pseudopotentials represented by the reciprocal space; and the valence electron configurations for elements were set as: Zn-3$d^{10}4s^2$, O-2$s^2 2p^4$, N-2$s^2 2p^3$, C-2$s^2 2p^2$ and H-1s^1. The cutoff energy for plane waves was determined by a of 340 eV, the numerical integration of the Brillouin zone was performed using a 2×2×1 Monkhorst-Pack *k*-point sampling, and the convergence tolerance for SCF was set as 1.0×10^{-6} eV/atom. The other calculation parameters and convergent criteria were set as the default values of the CASTEP code.

To better understand the reasons for the shift and quenching of the fluorescent spectra of two MOFs as the NACs were introduced, the frontier molecular orbitals for NACs and possible L-NACs complexes were predicted through DFT calculations by using the Gaussian09 suit of programs [3]. The hybrid meta-GGA density functional of M06-2X with addition of the D3 version of Grimme's dispersion were adopted, as was thought to give a good performance for the calculations of the weak interacting complexes [4-6]. And the all-electron 6-31G(d,p) basis sets were set for all atoms. All structures studied in this paper were fully optimized in the solvent using the Truhlar and co-workers' SMD [7] solvation model for the solvent effect correction of DMF.

References

[1] S. J. Clark, M. D. Segall, C. J. Pickard, P. J. Hasnip, M. J. Probert, K. Refson, M. C. Payne, *Zeitschrift fuer Kristallographie* 2005, **220**, 567-570.

[2] J. P. Perdew, K. Burke, M. Ernzerhof, *Phys. Rev. Lett.* 1996, **77**, 3865-3868.

[3] M. J. Frisch, G. W. Trucks, H. B. Schlegel, G. E. Scuseria, M. A. Robb, J. R. Cheeseman, G. Scalmani, V. Barone, B. Mennucci, G. A. Petersson, H. Nakatsuji, M. Caricato, X. Li, H. P. Hratchian, A. F. Izmaylov, J. Bloino, G. Zheng, J. L. Sonnenberg, M. Hada, M. Ehara, K. Toyota, R. Fukuda, J. Hasegawa, M. Ishida, T. Nakajima, Y. Honda, O. Kitao, H. Nakai, T. Vreven, J. A. Montgomery, Jr., J. E. Peralta, F. Ogliaro, M. Bearpark, J. J. Heyd, E. Brothers, K. N. Kudin, V. N. Staroverov, R. Kobayashi, J. Normand, K. Raghavachari, A. Rendell, J. C. Burant, S. S. Iyengar, J. Tomasi, M. Cossi, N. Rega, J. M. Millam, M. Klene, J. E. Knox, J. B. Cross, V. Bakken, C. Adamo, J. Jaramillo, R. Gomperts, R. E. Stratmann, O.

Yazyev, A. J. Austin, R. Cammi, C. Pomelli, J. W. Ochterski, R. L. Martin, K. Morokuma, V. G. Zakrzewski, G. A. Voth, P. Salvador, J. J. Dannenberg, S. Dapprich, A. D. Daniels, Ö. Farkas, J. B. Foresman, J. V. Ortiz, J. Cioslowski, and D. J. Fox, Gaussian, Inc., Wallingford CT, 2009.

[4] Y. Zhao, D. G. Truhlar, *Theor. Chem. Acc.* 2008, **120**, 215-241.

[5] S. Grimme, J. Antony, S. Ehrlich and H. Krieg, *J. Chem. Phys*., 2010, **132**, 154104.

[6] (a) Y. Zhao, D. G. Truhlar, Phys. *Chem. Chem. Phys.* 2008, **10**, 2813-2818. (b) S. N. Steinmann, G. Csonka, C. Corminboeuf, *J. Chem. Theory Comput.* 2009, **5**, 2950-2958. (c) S. N. Steinmann, C. Piemontesi, A. Delacht, C. Corminboeuf, *J. Chem. Theory Comput.* 2012, **8**, 1629-1640.

[7] A. V. Marenich, C. J. Cramer, D. G. Truhlar, *J. Phys. Chem. B* 2009, **113** 6378-6396.

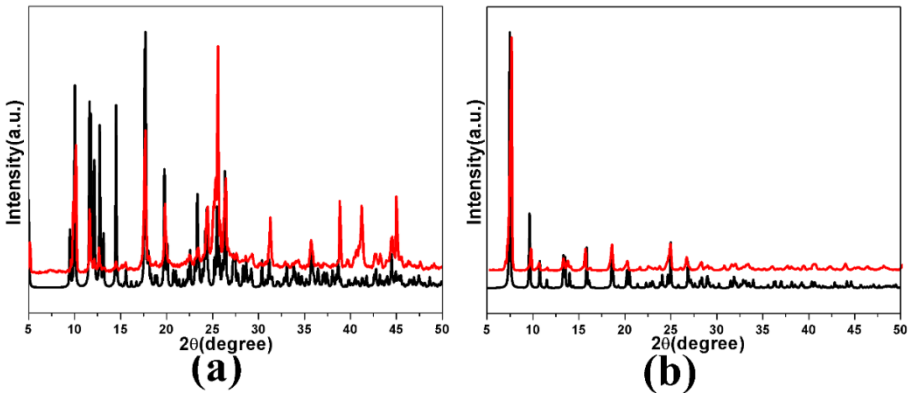

Fig. S1 The simulated (black) and experimental (red) PXRD patterns for the **1** (a) and **2** (b).

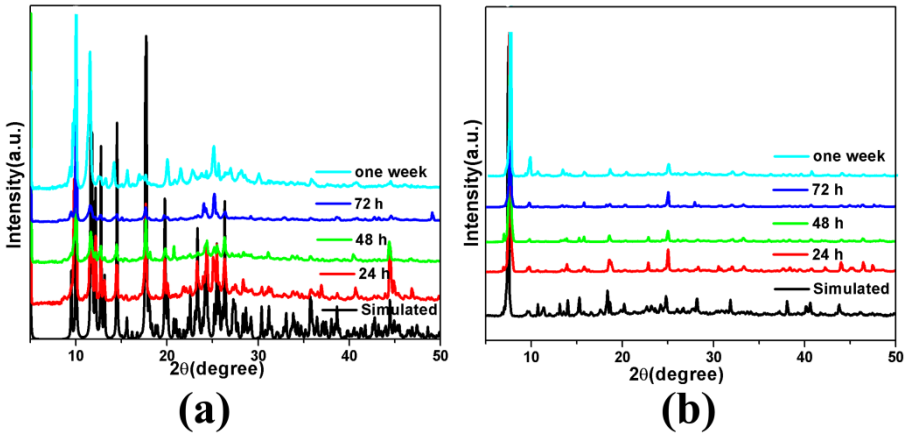

Fig. S2 PXRD patterns of **1** (a) and **2** (b) exposed to moist air with relative humidity of 60% for different times.

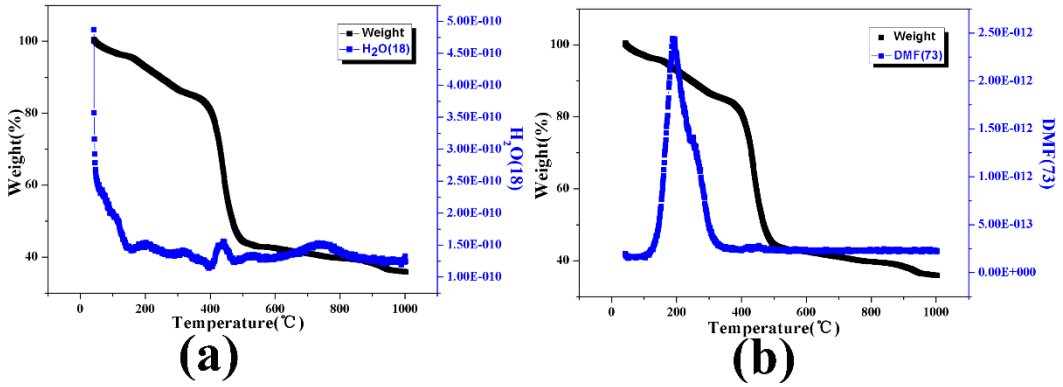

Fig. S3 Thermalgravimetricanalyzer-massspectrometry (TG-MS) data of **1**.

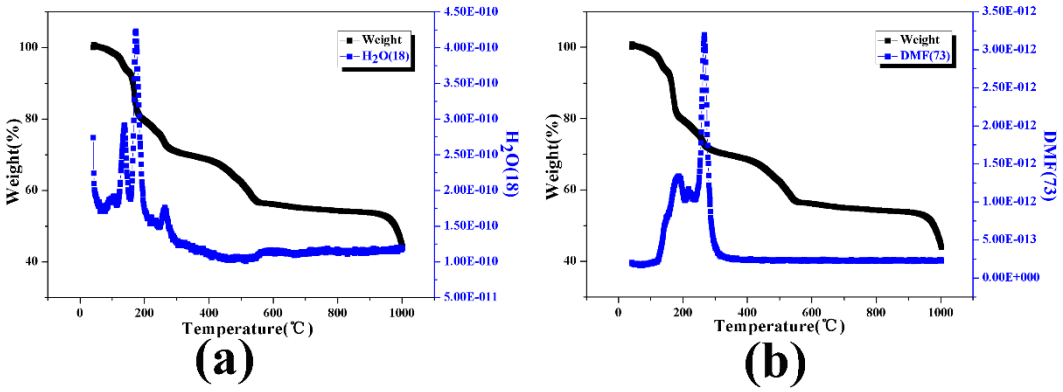

Fig. S4 Thermalgravimetricanalyzer-massspectrometry (TG-MS) data of **2**.

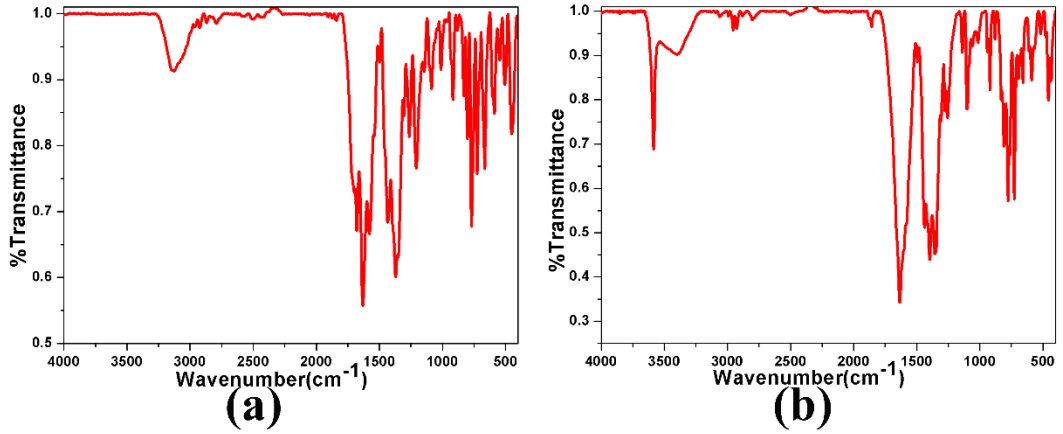

Fig. S5 IR spectra of **1** (a) and **2** (b).

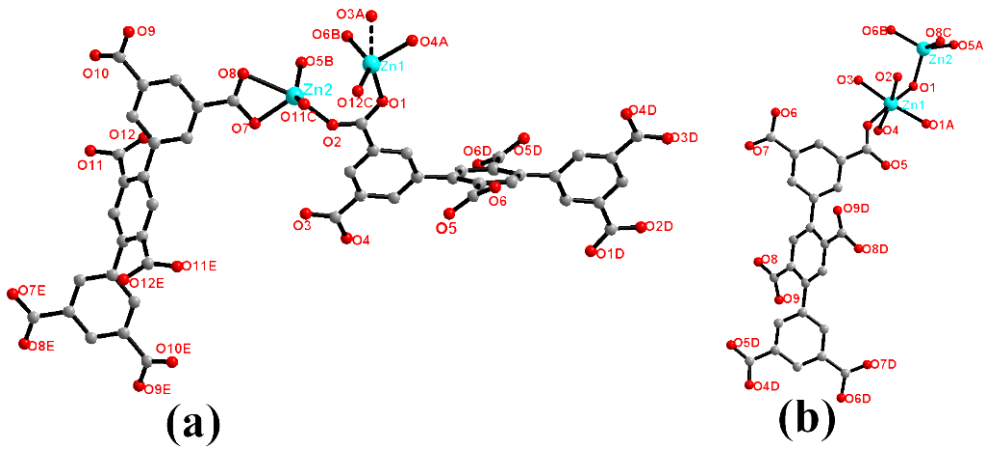

Fig. S6 The coordination environments for Zn(II) ions in **1** (a) and **2** (b).

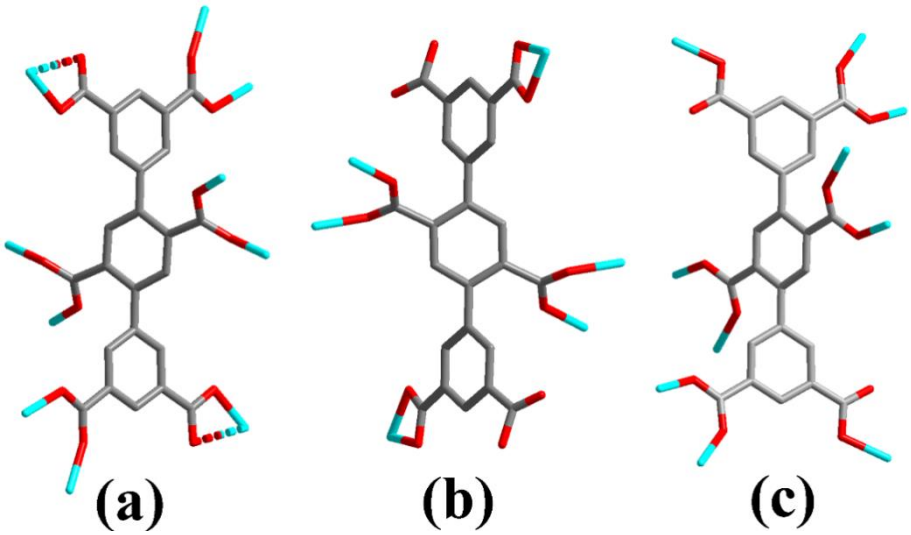

Fig. S7 The coordination modes of ligand in **1** (a, b) and **2** (c).

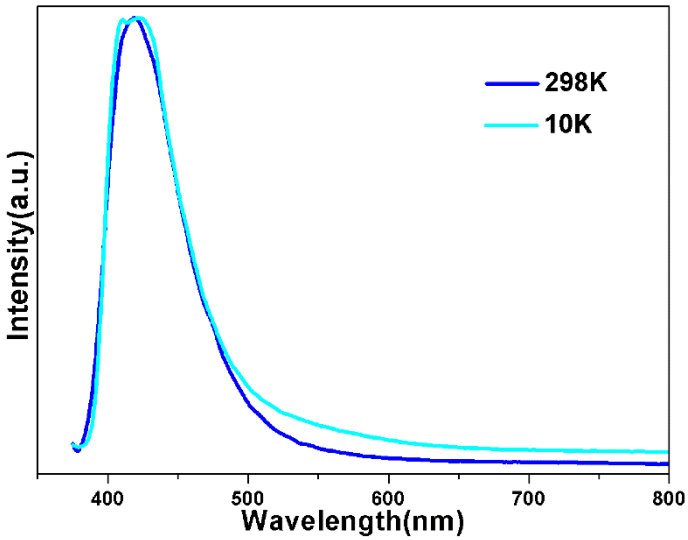

Fig. S8 Fluorescent spectra of free H_6L ligand at different temperatures.

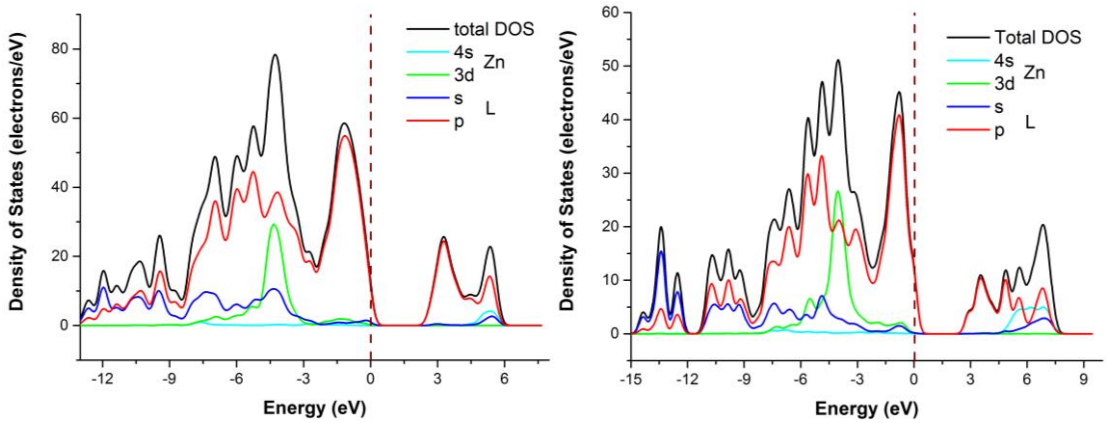

(a) (b)

Fig. S9 Total and partial DOS of complex **1** (a) and **2** (b). The position of the Fermi level is set at 0 eV.

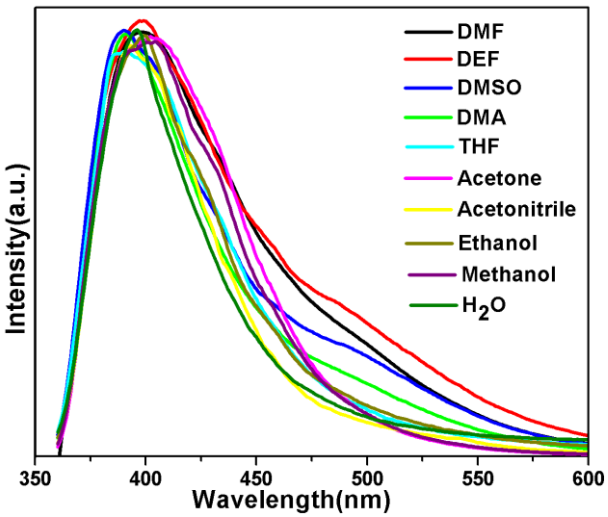

Fig. S10 Fluorescent spectra of complex **2** suspended in ten different solvents.

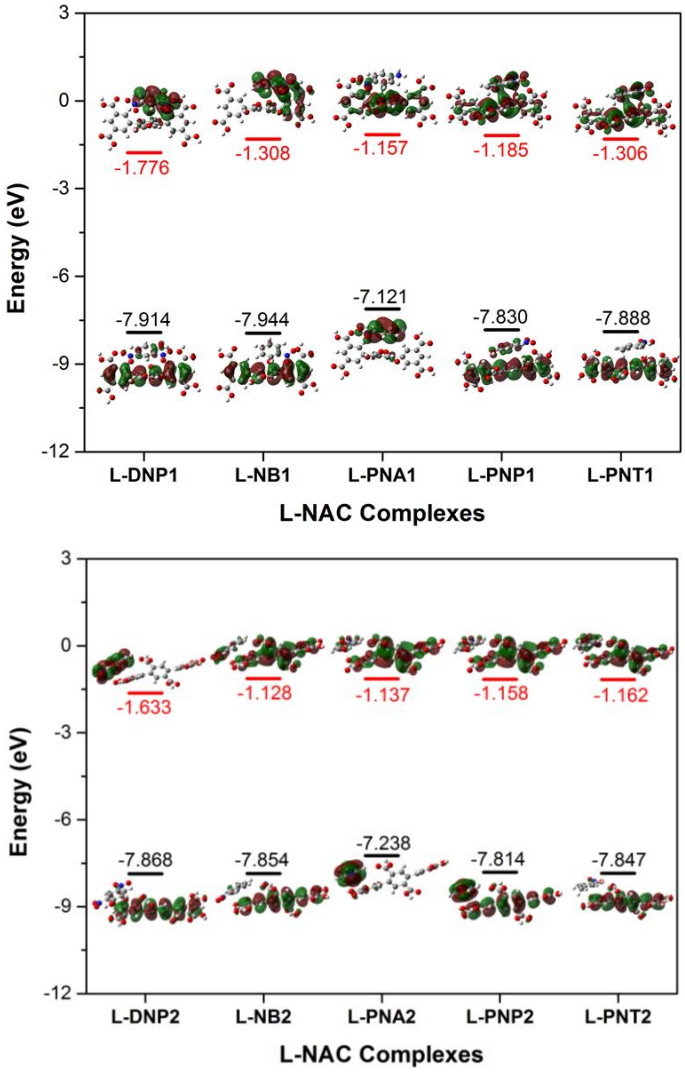

Fig. S11 The frontier molecular orbitals and the relative energies with solvent correction for the possible L-NAC complexes, which were investigated of at the M06-2X-GD3/6-31G(d,p) level of theory.

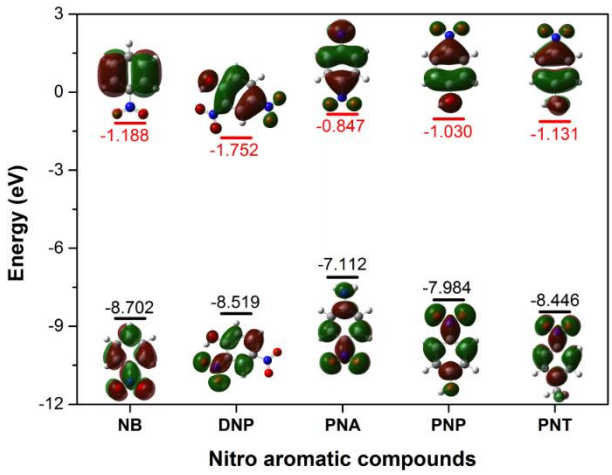

Fig. S12 The frontier molecular orbitals and the relative energies with solvent correction for the NACs, which were investigated at the M06-2X-GD3/6-31G(d,p) level of theory.

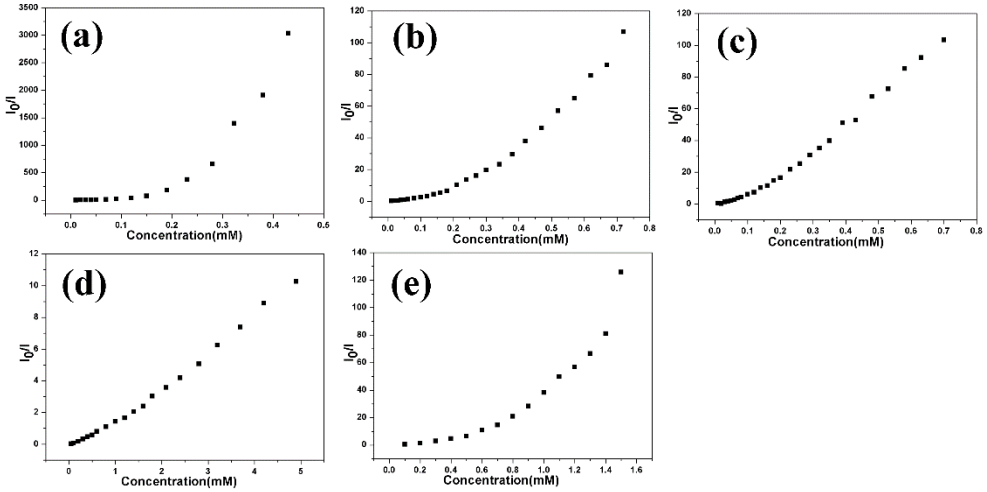

Fig. S13 The SV plots of **2** for (a) DNP; (b) PNP; (c) PNA; (d) PNT; (e) NB.

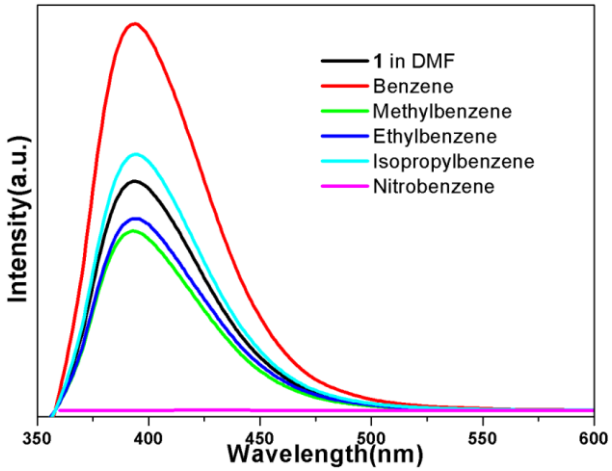

Fig. S14 The fluorescent spectra of **1** suspended in DMF with the addition of aromatic solvents.

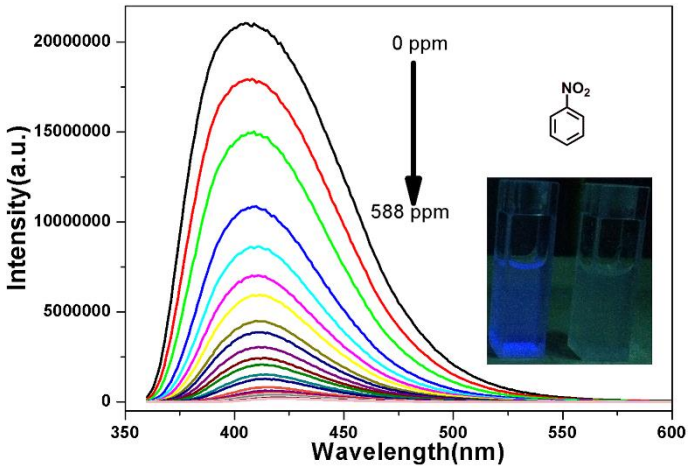

Fig. S15 Fluorescent quenching of **1** suspended in DMF with the gradual addition of NB.

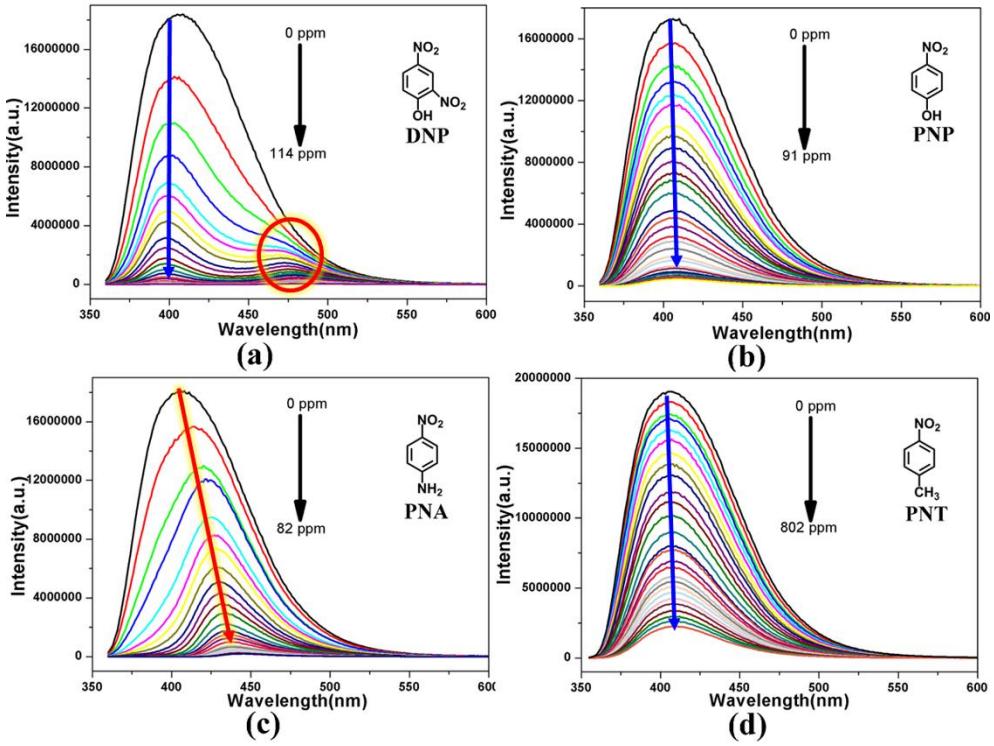

Fig. S16 Fluorescent spectra of **1** suspended in DMF with different NACs concentrations in DMF under λ_{ex}=345nm: (a) DNP; (b) PNP; (c) PNA; (d) PNT.

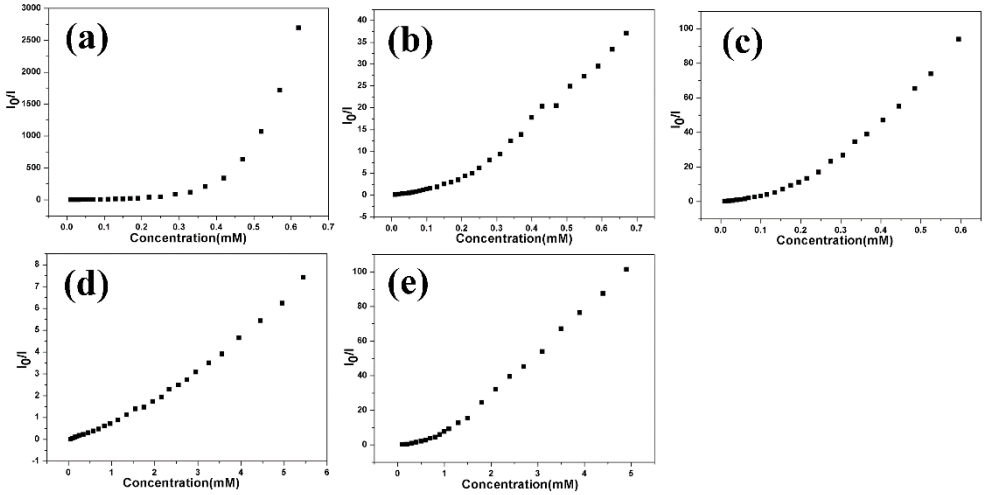

Fig. S17 The SV plots of **1** for (a) DNP; (b) PNP; (c) PNA; (d) PNT; (e) NB.

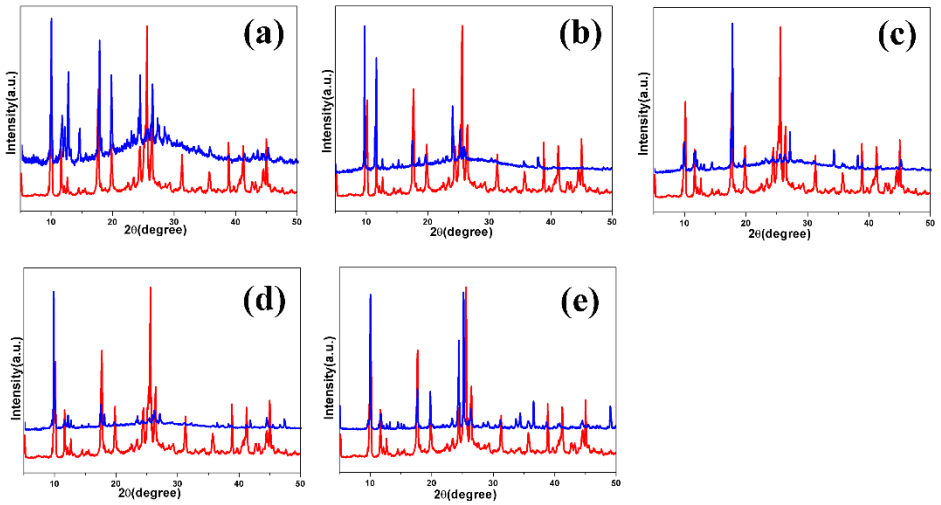

Fig. S18 PXRD patterns of **1** before (red) and after detection experiments (blue): (a) DNP; (b) PNP; (c) PNA; (d) PNT; (e) NB.

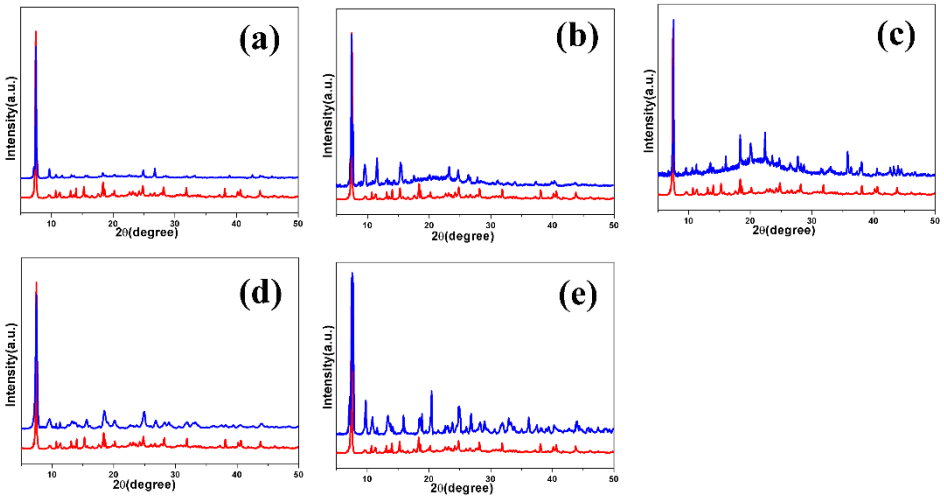

Fig. S19 PXRD patterns of **2** before (red) and after detection experiments (blue): (a) DNP; (b) PNP; (c) PNA; (d) PNT; (e) NB.

Table S1. CIE coordinates of **2** at different temperatures.

Temperature	Coordinate	Temperature	Coordinate
290 K	0.24,0.30	130 K	0.29,0.51
270 K	0.25,0.35	110 K	0.29,0.51
250 K	0.27,0.41	90 K	0.29,0.52
230 K	0.27,0.43	70 K	0.29,0.52
210 K	0.28,0.46	50 K	0.29,0.52
190 K	0.29,0.48	30 K	0.29,0.52
170 K	0.29,0.49	10 K	0.29,0.52
150 K	0.29,0.50		

Table S2 The concentrations of different NACs when significant and completely quenching occurred for **1.**

	Significant Quenching (QE = 50%)	**Completely Quenching (QE = 97%)**
DNP	5ppm	40 ppm
PNA	7ppm	46 ppm
PNP	12ppm	85 ppm
NB	48ppm	288 ppm
PNT	185ppm	800 ppm (QE = 88%)

Table S3. Crystal Data and Structure Refinements for complexes **1-2**.

Complexes	**1**	**2**
Empirical formula	$C_{58}H_{52}N_4O_{28}Zn_4$	$C_{30}H_{32}N_2O_{20}Zn_4$
Formula weight	1514.68	1002.21
Temperature (K)	100 (2)	173 (2)
Crystal system	Triclinic	Triclinic
Space group	*P*-1	*P*-1
a [Å]	8.5170(4)	7.8732(4)
b[Å]	10.3341(4)	9.6571(4)
c [Å]	18.2392(7)	12.1461(6)
α [^{o}]	104.782(4)	76.894(4)
β [^{o}]	91.187(3)	89.325(4)
γ [^{o}]	110.479(4)	77.575(4)
V [Å^3]	1443.34(11)	877.71(7)
Z	2	1

Dc[g/cm^{-3}]	1.701	1.892
μ [mm^{-1}]	2.702	3.908
F(000)	752	504
θ range(°)	4.7–73.3	4.8–72.9
GOF on F^2	1.047	1.028
Parameters	420	255
R_1(I >2σ(I))[a]	0.0368	0.0270
wR_2(I >2σ(I))[b]	**0.0966**	**0.0785**

Table S4. The calculated distances (Z) between two offset benzene rings as the π-π interaction parameters for possible L-NAC complexes.

	L-NB1	**L-DNP1**	**L-PNA1**	**L-PNP1**	**L-PNT1**
Z / Å	3.7224	3.7093	3.7187	3.5365	3.6406
	L-NB2	**L-DNP2**	**L-PNA2**	**L-PNP2**	**L-PNT2**
Z / Å	3.6377	3.5920	4.0157	3.7817	3.7897

Table S5. The forntier molecular orbital energies for NACs and possible L-NAC complexes, as calculated at M06-2X-GD3/6-31G** level of theory.

	HOMO / eV	**LUMO / eV**	**Energy Gap /eV**
NB	-8.702	-1.188	7.514
DNP	-8.519	-1.752	6.767
PNA	-7.112	-0.847	6.266
PNP	-7.984	-1.030	6.955
PNT	-8.446	-1.131	7.315
L	-7.875	-1.138	6.737
L-DNP1	-7.912	-1.773	6.139
L-DNP2	-7.867	-1.633	6.234
L-NB1	-7.944	-1.309	6.635
L-NB2	-7.854	-1.128	6.726
L-PNA1	-7.121	-1.157	5.964
L-PNA2	-7.238	-1.137	6.101
L-PNP1	-7.830	-1.185	6.645
L-PNP2	-7.814	-1.158	6.656
L-PNT1	-7.888	-1.306	6.582
L-PNT2	-7.847	-1.162	6.685

Table S6. Selected Bond Lengths (Å) and Bond Angles (°) for Complexes **1**-**2**.

Complex 1			
Bond	Dist.	Bond	Dist.
Zn1—O12^{i}	1.9390 (19)	Zn2—O5^{iii}	1.968 (2)
Zn1—O4^{ii}	1.9646 (19)	Zn2—O7	2.0062 (18)
Zn1—O6^{iii}	1.9648 (19)	Zn2—O2	2.0180 (19)
Zn1—O1	2.000 (2)	Zn2—O8	2.2917 (18)
Zn2—O11^{i}	1.9581 (19)		
Angle	(°)	Angle	(°)
O12^{i}—Zn1—O4^{ii}	108.15 (8)	O7—Zn2—O2	102.13 (8)
O12^{i}—Zn1—O6^{iii}	133.51 (9)	O11^{i}—Zn2—O8	96.32 (7)
O4^{ii}—Zn1—O6^{iii}	107.90 (8)	O5^{iii}—Zn2—O8	87.17 (8)
O12^{i}—Zn1—O1	97.77 (9)	O7—Zn2—O8	61.05 (7)
O4^{ii}—Zn1—O1	109.25 (8)	O2—Zn2—O8	162.12 (8)
O6^{iii}—Zn1—O1	97.08 (9)	O11^{i}—Zn2—C13	104.84 (8)
O11^{i}—Zn2—O5^{iii}	141.39 (9)	O5^{iii}—Zn2—C13	97.10 (8)
O11^{i}—Zn2—O7	107.13 (8)	O7—Zn2—C13	31.30 (8)
O5^{iii}—Zn2—O7	108.07 (8)	O2—Zn2—C13	132.91 (8)
O11^{i}—Zn2—O2	94.60 (8)	O8—Zn2—C13	29.81 (8)
O5^{iii}—Zn2—O2	93.09 (9)		
Symmetry codes: (i) -1+x, -1+y, z; (ii) x, -1+y, z; (iii) 1+x, -1+y, z.			

Complex 2			
Bond	Dist.	Bond	Dist.
Zn1—O4	2.0673 (18)	Zn1—O3	2.1199 (18)
Zn1—O1^{i}	2.0861 (17)	Zn2—O6^{iii}	1.9326 (18)
Zn1—O1	2.1058 (17)	Zn2—O5^{i}	1.9553 (18)
Zn1—O2	2.1139 (19)	Zn2—O1	1.9696 (17)
Zn1—O9^{ii}	2.1169 (18)	Zn2—O8^{iv}	1.9724 (18)
Angle	(°)	Angle	(°)
O4—Zn1—O1^{i}	98.19 (7)	O1^{i}—Zn1—O3	169.66 (8)
O4—Zn1—O1	171.99 (7)	O1—Zn1—O3	89.20 (7)
O1^{i}—Zn1—O1	80.56 (7)	O2—Zn1—O3	88.27 (8)
O4—Zn1—O2	87.72 (7)	O9^{ii}—Zn1—O3	85.13 (7)
O1^{i}—Zn1—O2	94.91 (7)	O6^{iii}—Zn2—O5^{i}	125.66 (8)
O1—Zn1—O2	100.26 (7)	O6^{iii}—Zn2—O1	104.48 (8)
O4—Zn1—O9^{ii}	85.72 (7)	O5^{i}—Zn2—O1	108.49 (7)
O1^{i}—Zn1—O9^{ii}	92.77 (7)	O6^{iii}—Zn2—O8^{iv}	109.85 (8)
O1—Zn1—O9^{ii}	86.44 (7)	O5^{i}—Zn2—O8^{iv}	101.03 (8)
O2—Zn1—O9^{ii}	170.54 (7)	O1—Zn2—O8^{iv}	106.02 (7)
O4—Zn1—O3	91.76 (8)		
Symmetry codes: (i) -x, -y, 1-z; (ii) 1-x, -y, 2-z; (iii) -x, 1-y, 1-z; (iv) -1+x, y -1+z.			